AS4.6-EGU2020-375

Moisture Source-to-Receptor Network for the East Asian Summer Monsoon Land Regions

Tat Fan Cheng[1] and Mengqian Lu[1,*]

[1]: Department of Civil and Environmental Engineering, The Hong Kong University of Science and Technology, Hong Kong, China

Presenting Author: Tat Fan Cheng (tfchengac@connect.ust.hk); Corresponding Author (*): Mengqian Lu (mengqian.lu@ust.hk)

Motivations

Given the profound socioeconomic impacts of the East Asian Summer Monsoon (EASM), there has been growing interest in studying the moisture sources involved, which represents a crucial component of the water cycle connecting the monsoon system. As various pieces of literature debated on different predominant sources from Indian, Pacific, Eurasian or even local areas, our understanding of the moisture-to-receptor (SR) network for the EASM remains ambiguous yet. To quantify the moisture sources, we employ a 2D dynamic recycling model (DRM). It is a semi-Lagrangian model derived solely from the atmospheric water budget equation and allows computationally efficient estimations on the moisture sources with good fidelity (Martinez and Dominguez 2014), especially when the atmosphere over East Asia and adjacent seas is largely well-mixed [See Figure 3b and 4b in Goessling & Reick (2013)].

Goals

- Establish a complete SR network for the EASM land regions
- Identify the governing circulations for the SR network during heavy rainfall days
- Explore the potential influence of the El Niño-Southern Oscillation (ENSO) on the SR network

Data & Methods

Table 1. Important equations/variables related to the DRM.

Variable	Description	Equation
Recycling ratio (R)	Fraction of precipitation recycled from evapotranspiration (E) considering precipitable water (W)	$R = 1 - exp\left[-\int_0^\tau \frac{E}{W}\,d\tau'\right]$
	Sum of relative contributions from each source along the trajectory	$R = R_1 + (1-R_1)R_2 + (1-R_1)(1-R_2)R_3 + \cdots$
$\overline{P_m}$	Area-weighted amount contribution of precipitation from region A_k to region A_i at time t	$\overline{P_m}(A_k, A_i, t) = \frac{\sum_{(x,y)\in A_i} R(x,y,t,A_k)\times P(x,y,t)\times \delta A(x,y)}{\sum_{(x,y)\in A_i} \delta A(x,y)}$
$\bar{R}$	Regional recycling ratio over a period T	$\bar{R}(A_k, A_i) = \frac{\int_0^T \overline{P_m}(A_k, A_i, t)\,d\tau}{\int_0^T P(A_i, t)\,d\tau}$

- A 40-year hourly data (1979-2018) is retrieved from the ERA5 reanalysis with 0.25°×0.25° spatial resolution. We choose April to September to capture the sources from pre-monsoon to post-monsoon periods.
- Full-fledged ENSO events are classified based on a threshold of ±0.5°C in the Oceanic Niño Index for at least five consecutive months, as suggested by the Climate Prediction Center.

Results

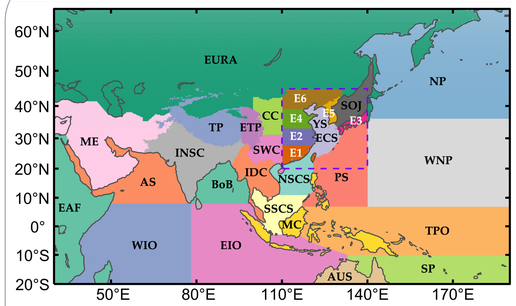

Fig. 1. Prescribed 30 regions in the DRM. E1 to E6 represents the EASM land subregions and are set as sink regions in the model.

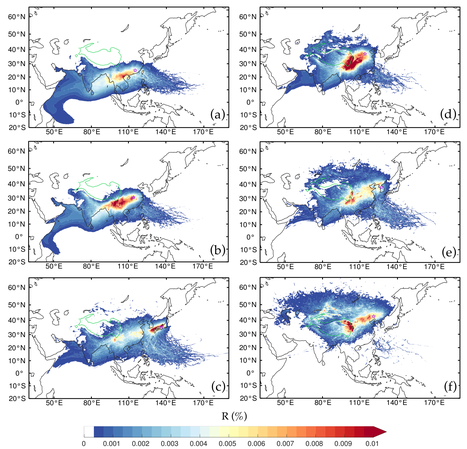

Fig. 2. Wet season climatology (April to September) of the ratio contribution (%) in (a) E1 to (f) E6 region.

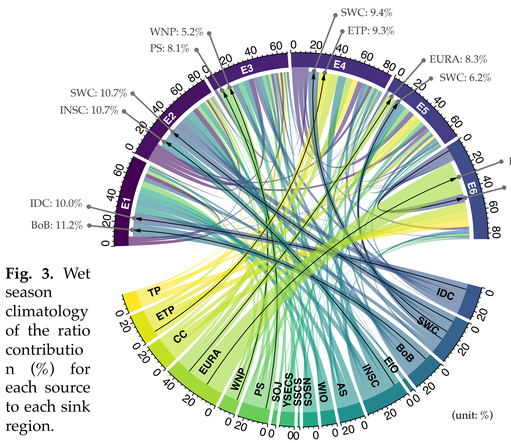

Fig. 3. Wet season climatology of the ratio contribution (%) for each source to each sink region.

Climatology

66-72% of the precipitation over EASM land regions are attributed by the back-trajectory model (i.e., DRM). Major moisture routes are from Indian, Pacific and Eurasian areas (Fig. 2). For each sink regions, the highest recycling ratios are found to the southwest, showing the importance of the summer monsoons. Further quantification reveals the importance of land sources (Fig. 3).

SW-to-SE transition

Figure 4 unveils a shift in dominant sources from southwesterly to southeasterly sectors on intraseasonal time scale. For example, E1 receives moisture mostly from Indochina, Indian peninsula, Bay of Bengal and Arabian Sea from April to June. Since July, Pacific sources from the southeast rise as the leading moisture supplier (Fig. 4a). The transition is even salient by distinguishing sources by oceans and continents (Fig. 4g, h)

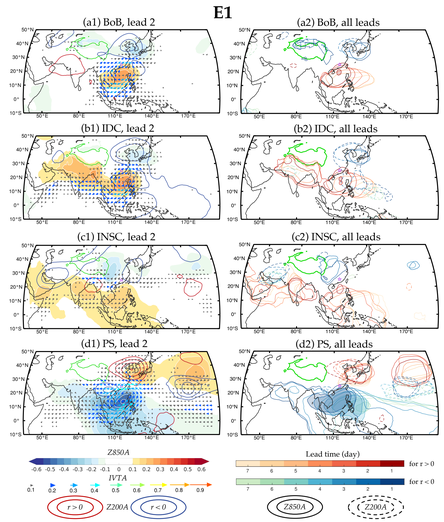

Fig. 5. Lead-lag correlation map (Spearman's rho) of the amount contribution anomalies of (a) BoB, (b) IDC, (c) INSC and (d) PS for the E1 subregion with different meteorological variables during its heavy rainfall days. Panel (1) shows the time lag with the strongest lead-lag correlation fields of Z850A (shaded), Z200A (contour; interval: 0.05 starting from ±0.1) and IVTA (vector). Panel (2) depicts the lead-lag correlations for Z850A (solid) and Z200A (dashed) at lead times from 1 to 7 days, with correlations of 0.15 (contour) and 0.3 (shaded) shown only. All correlations shown are statistically significant at the 0.05 level.

Governing Circulations

Based on the lead-lag one-point correlation map during heavy rainfall days (top15%), a westward propagating pressure anomaly is associated with enhanced contributions from South Asian and Indian sources (Fig. 5a2, b2). Conversely, a cyclonic circulation anomaly is related to more moisture supply from Philippine Sea (Fig. 5d2). These are likely due to the zonal oscillation of the subtropical high.

Further, northeast (NE)-type and northwest (NW)-type pressure dipoles are noted. The former tends to steer moisture from nearby sources (Fig. 5a, b, d), while the latter supports long-range moisture routes reaching to the Indian peninsula (Fig. 5c).

Intriguingly, we find wave trains from the western Russia to East Asia, which are the key drivers for the moisture supply from Indian Peninsula and eastern Tibetan Plateau to the E4 subregions (Fig. 6). We speculate that such upper-level wave trains creates divergent circulation in which rising motion is triggered and thus lead to depression and the corresponding moisture routes at lower-levels. All the above circulations are also seen in SR pairs related to other sink regions (not shown).

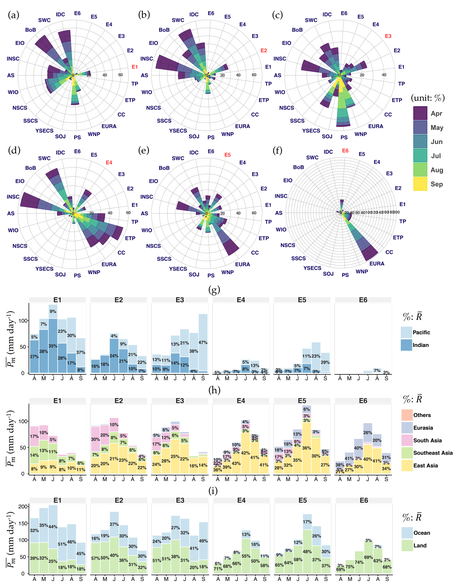

Fig. 4. Monthly climatology of the ratio contribution (%) from sources to (a) E1 to (f) E6 region, and sources in categories of (g) Pacific Ocean and Indian Ocean, (h) Eurasia, South Asia, Southeast Asia, East Asia and the other land regions, and (i) ocean and land regions.

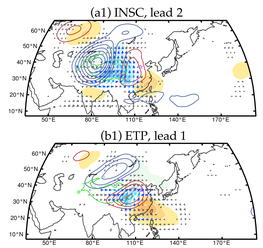

Fig. 6. As the panel 1 in Fig. 5, but for the sources to the E4 subregion.

Wintertime ENSO

Moisture supply from Indian basin and the Southwest China is significantly enhanced under the scenario of an El Niño event in the preceding winter (by Kolmogorov–Smirnov test) (Fig. 7a, c-e). An anomalous high-pressure band could account for this lag impact (not shown).

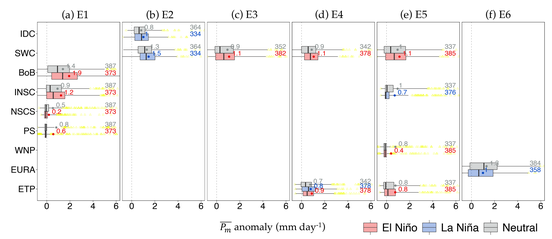

Fig. 7. Boxplots of the amount contribution anomalies (mm day^{-1}) during heavy rainfall days of (a) E1 to (f) E6 under the context of ENSO events in the preceding winter.

Reference

Martinez, J. A., and F. Dominguez, 2014: Sources of Atmospheric Moisture for the La Plata River Basin*. J. Clim., 27, 6737–6753, doi:10.1175/JCLI-D-14-00022.1.

Goessling, H. F., and C. H. Reick, 2013: On the "well-mixed" assumption and numerical 2-D tracing of atmospheric moisture. Atmos. Chem. Phys., 13, 5567–5585, doi:10.5194/acp-13-5567-2013.